

EDGE-ROUNDED MAGNET POLES FOR REDUCING THE TORQUE RIPPLE ON A RADIAL FLUX INSET PERMANENT MAGNET GENERATOR

Wike Handini¹, Rudy Setiabudy¹, Ridwan Gunawan¹, Chairul Hudaya^{1*}

¹*Department of Electrical Engineering, Faculty of Engineering, Universitas Indonesia, Kampus UI Depok 16424, Indonesia*

(Received: May 2016 / Revised: February 2017 / Accepted: January 2018)

ABSTRACT

This study reports a novel strategy for minimizing torque ripple in a radial flux inset permanent magnet (RFIPM) generator by using a geometric modification of the magnet poles. We simulate the design of three different types of edge-rounded magnet (ERM) poles using finite element method magnetics (FEMM) software for a 16 poles and 24 slots RFIPM generator. We found that the edge-rounding of magnet poles significantly lowered the torque ripple of the generator with a reduction of about 74% (torque ripple of 7.76%). In addition, the modified RFIPM generator exhibited enhanced flux density uniformity in the air-gap of the generator (up to ~ 48.8%), leading to a smoother line of flux density.

Keywords: Edge-rounded magnet poles; Finite element method magnetic; Flux density uniformity; Radial flux inset permanent magnet generator; Torque ripple reduction

1. INTRODUCTION

Permanent magnets have been widely used in electrical machines, such as motors and generators, since they improve the efficiency and reliability of the machines due to the absence of excitation losses (Yicheng et al., 2005; Gieras, 2010). Moreover, electrical machines using permanent magnets such as direct-drive permanent magnet machines have other advantages compared to gear box-based machines, including higher reliability and efficiency, less maintenance, less noise and as low weight (Meier, 2008). One of the main challenges in designing a permanent magnet-based generator is the torque quality. Torque distortion such as cogging torque and torque ripple may cause a magnetic vibration and noise. This distortion may be transmitted directly to the load and drive shaft, degrading the lifetime of the electric machines (Islam et al., 2009). Torque ripple is mostly caused by the non-homogeneous distribution of flux density in the air-gap of the generator due to the interaction of the current fundamental harmonic and the EMF harmonics (Gasc et al., 2003).

Several studies have been devoted to overcome the aforementioned problems. In general, there are two approaches for reducing torque ripple. The first strategy is to improve the magnetic design of the electric machines by changing the geometry of the stator and rotor poles. The other one is to use the electronic control technique, which is based on control parameters such as supply voltage, turn-on and turn-off angles, and current level (Husain, 2002, Sunan et al., 2010). Compared to the latter technique, the former method is more desirable because it may effectively reduce torque ripple, whereas the electronic control technique requires a precise real-time excitation current, according to the real-time computations. In addition, real-time

*Corresponding author's email: c.hudaya@eng.ui.ac.id, Tel: +62-21-7270078, Fax: +62-21-7270077
Permalink/DOI: <https://doi.org/10.14716/ijtech.v9i3.1906>

computation is very sensitive in terms of the reliability and accuracy of the sensors used in the control system (Weizhong et al., 2011).

Ahsanullah et al. proposed a method for optimization for the reduction torque ripple and cogging torque by changing the magnet arcs and choosing an optimum flux barrier in the interior permanent magnet machine using two-dimensional finite element analysis (Ahsanullah et al., 2013). Using this method, they successfully decreased the cogging torque to be less than 1%. Another approach involved using a multilayer structure for stator windings and changing the rotor geometry (Alberti et al., 2014). The authors reported a torque ripple lower than 1.5% at full load. An asymmetric flux barrier and asymmetric lamination method was proposed by Ki-Chan Kim to reduce torque ripple and cogging torque (Ki-Chan, 2014). Their effort resulted in an asymmetric barrier in a permanent magnet rotor without permanent magnet skew. A similar approach by Dajaku and Gerling reduced torque ripple through a new stator design with right- and left-shifted slot openings to minimize the cogging torque (Dajaku & Gerling, 2014). Upadhayay and Rajagopal used the magnet pole shaping technique for torque ripple reduction on a 12 poles and 18 slots surface mounted permanent magnet brushless DC motor (Upadhayay & Rajagopal, 2013). The performance parameters were computed and analyzed by two-dimensional finite element analysis. Gyeong-Chan et al. proposed a design of pole arc and permanent magnet structure to reduce cogging torque and torque ripple for an outer rotor radial flux surface mounted permanent magnet generator (Gyeong-Chan et al., 2014). Nur and Haroen investigated the influence of a magnet pole slot of 6 poles and 18 slots of an inset permanent magnet synchronous machine on cogging torque. They found that slotting the edge of the magnet reduced the cogging torque effectively (Nur & Haroen, 2014). Recently, our group successfully simulated the combination of ERM and stator teeth notch techniques with optimum parameters and found that the torque ripple was significantly reduced up to 80% (Handini et al. 2016).

In this paper, we investigate the effect of edge-rounding of permanent magnet poles on torque ripple reduction of a 16 poles and 24 slots radial flux inset permanent magnet (RFIPM) generator. We simulated the system using FEMM software and found the proposed method effectively decreases the torque ripple and improves the uniformity of electromagnetic flux density.

2. TORQUE RIPPLE

The electromagnetic torque of electric machines has two main torque components, and is expressed as (Gieras, 2010):

$$T(\alpha) = T_0 + T_r(\alpha) \quad (1)$$

where T_0 is a constant or average component and $T_r(\alpha)$ is a periodic component, which is a function of time or angle α . The periodic component causes the torque pulsation called torque ripple. Torque ripple is given by (Gieras, 2010):

$$t_r = \frac{T_{\max} - T_{\min}}{T_{\text{av}}} \quad (2)$$

where

$$T_{\text{av}} = \frac{1}{T_p} \int_{\alpha}^{\alpha+T_p} T(\alpha) d\alpha = \frac{1}{T_p} \int_0^{T_p} T(\alpha) d\alpha \quad (3)$$

and T_p is the period of the torque waveform.

3. EXPERIMENTAL DETAILS

We are interested in a RFIPM generator with 16 poles and 24 slots because this typical generator is mainly used for a low-speed wind power system. In this study, we designed three different models of edge-rounded magnet (ERM) poles. Figure 1 shows the cross-section view of the basic model and the respective developed ERM model of the RFIPM generator. The main parameters are presented in Table 1.

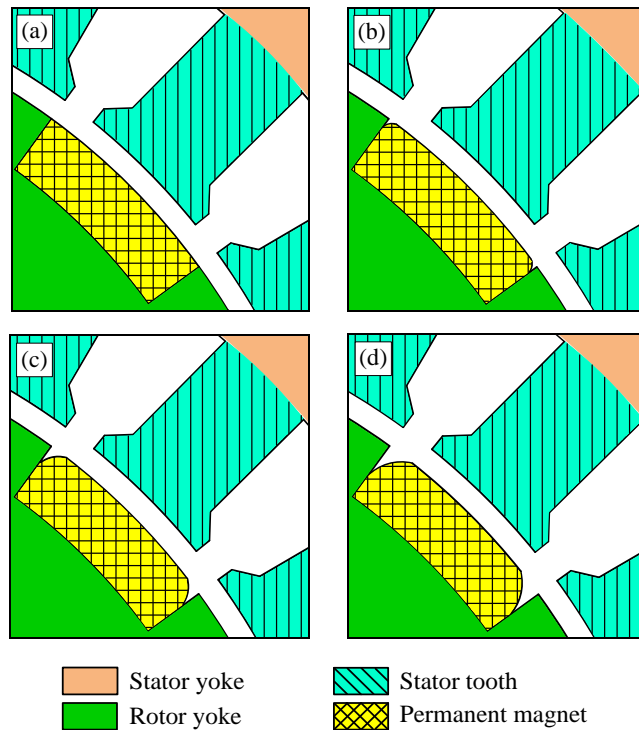


Figure 1 Cross-sectional view of RFIPM generator for (a) basic model; (b) ERM 1; (c) ERM 2; (d) ERM 3

Table 1 Parameters of RFIPM generator

Parameters (1)	Symbols (2)	Value (3)	Unit (4)
Number of slots	Q_s	24	-
Number of poles	p	16	-
Stator outer radii	r_{so}	102	mm
Stator inner radii	r_{si}	71	mm
Rotor outer radii	r_{ro}	70	mm
Rotor inner radii	r_{ri}	65	mm
Magnet pole thickness	l_{pm}	5	mm
Air gap length	g	1	mm
Pole arc/pitch ratio	α	0.80	-

Since the geometric modification of magnet poles does not change their thickness and width, the cross-section area of the ERM models are slightly smaller than that of the basic model owing to the removal of the magnet material. This phenomenon causes a higher air gap volume in the ERM models compared to their basic counterpart. The cutting residue in the ERM poles Δ (mm^2) is identified by blue color in Figure 2.

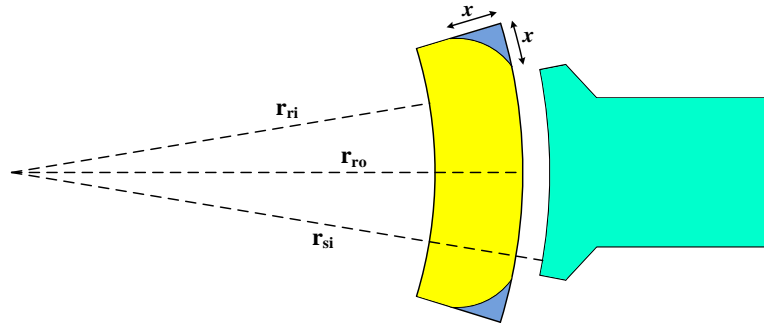


Figure 2 Cross section area of magnet cut

The cross-section area of magnet cut is obtained using the following equation:

$$\Delta = x r_{ro} - \left(r_{ro} (r_{ro} - x) \sin\left(\frac{x}{r_{ro}}\right) \right) - \frac{2\pi - 3\sqrt{3}}{6} \left[\left(r_{ro} - (r_{ro} - x) \cos\left(\frac{x}{r_{ro}}\right) \right)^2 + \left((r_{ro} - x) \sin\left(\frac{x}{r_{ro}}\right) \right)^2 \right] \quad (4)$$

where r_{ro} is the rotor outer radii of an RFIPM generator (mm) and x is the length of the magnet cut (mm). Using Equation 4, we can find the three ERM models' cross-section area (A_{magnet}) by the following equation:

$$A_{\text{magnet}} = \frac{\alpha \pi (r_{ro}^2 - r_{ri}^2)}{p} - \Delta \quad (5)$$

and the cross-section area of the air gap (A_{gap}) is given by:

$$A_{\text{gap}} = \pi (r_{si}^2 - r_{ro}^2) + \Delta \quad (6)$$

where p is the numbers of poles, α is the pole arc/pitch ratio, r_{si} is the stator inner radii (mm) and r_{ri} is the rotor inner radii (mm) of RFIPM. From this equation, we can calculate the volume of the magnet pole and air-gap as well, as shown in Table 2.

Table 2 Calculated volume of 1 magnet pole and air-gap in generator

Parameters	Symbols	Basic model	ERM 1	ERM 2	ERM 3	Unit
Volume of 1 magnet pole	A_{magnet}	8,058	8,009	7,861	7,612	mm ³
Air gap volume	A_{gap}	33,665	34,447	36,815	40,804	mm ³

4. RESULTS AND DISCUSSION

In this paper, we simulate an RFIPM generator with the basic model and three types of magnet shapes (ERM 1, ERM 2, and ERM 3) using FEMM 4.2. During the simulation, the rotor position is gradually turned for every 1° starting from 0° to 45°. The torque ripple obtained by simulation is plotted in Figure 3. The maximum torque ripples for the basic model, ERM 1, ERM 2, and ERM 3 are 69.7, 66.6, 62.3, and 66.7 Nm, respectively. Figure 4 shows the values of the torque ripple RFIPM generator calculated using Equation 2. We found that the developed ERM models exhibited a lower torque ripple than that of the basic one. The lowest torque ripple was achieved by ERM 2 (7.76%), followed by ERM 1 (21.68%), ERM 3 (22.30%), and the basic model (29.87%).

It is interesting to compare our results with those of other studies available in the literature. Although the systems in these studies differ with respect to the employed methods, the value of torque ripple produced by our design is lower than those achieved by Ki-Chan Kim (9.33%), Upadhayay and Rajagopal (16.89%), Jiang et al. (9.6%), and Baek et al. (9.96%) (Ki-Chan, 2014, Upadhayay and Rajagopal, 2013, Jiang et al., 2014, Baek et al., 2014). Our result is still slightly higher than that reported by Gyeong-Chan et al. (4.3%), Kyung-Sik et al. (2.16%), and Daohan et al. (2.73%) (Gyeong-Chan et al., 2014, Kyung-Sik et al., 2014, Daohan et al., 2013). Nevertheless, the low torque ripple obtained by Daohan et al. was worsened with unbalanced magnetic pull due to the asymmetric distribution of the magnets (Daohan et al., 2013).

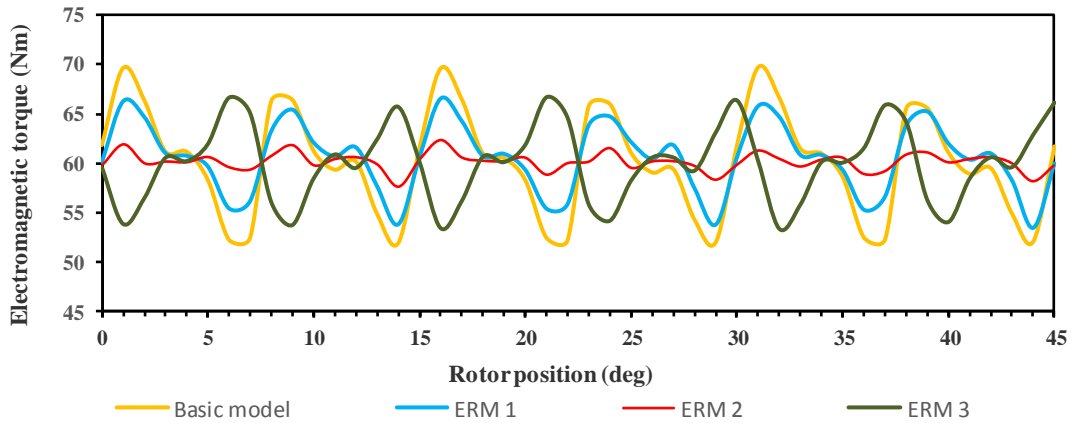


Figure 3 Electromagnetic torque of RFIPM generator for basic shape and proposed models

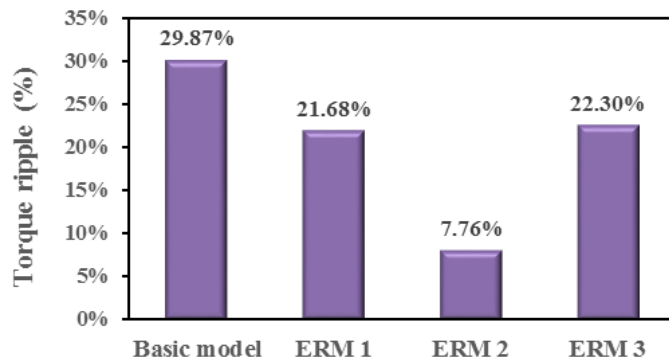


Figure 4 Comparison of torque ripple of basic model and ERM poles of RFIPM generator

The distribution of magnetic flux density in the air-gap for the basic model and proposed models is presented in Figure 5. The lines of flux density are circulated in the air-gap from the magnets to the stator teeth and eventually returned back to the magnets. In order to distinguish the phenomena in the RFIPM during the operation, we indicate the flux ripples using red circles in Figure 5. As can be seen, for the basic model, the flux line is much more distorted compared with the ERM models. Among the proposed models, ERM 2 exhibits the smoothest flux line, followed by ERM 1 and ERM 3. This result is in good agreement with the torque ripple reduction presented in Figure 6. With respect to the basic model, the torque ripple reduction of ERM 2, ERM 1, and ERM 3 was 74.02%, 27.42%, and 25.34%. We also correlated the reduction in magnet volume and the increment of the air-gap volume. Although the increasing values of those parameters tended to decrease the torque ripple, we found that the parameter values should be optimized.

Flux density uniformity (B_{UNI}) is closely related to the torque ripple and is expressed as:

$$B_{UNI} = \frac{B_{max} - B_{min}}{2B_{av}} \times 100\% \quad (7)$$

where B_{max} , B_{min} , and B_{av} are the maximum, minimum, and average electromagnetic flux values, respectively. A lower B_{UNI} is desired, representing a small deviation among the electromagnetic flux. In contrast, higher B_{UNI} indicates a high difference between B_{max} and B_{min} , which should be avoided.

Figure 7 shows the uniformity of electromagnetic flux density, computed using Equation 7. The best flux density uniformity was achieved by ERM 2 (48.8%), followed by ERM 1, ERM 3 and basic model. These results are in good agreement with the torque ripple explained in the previous section.

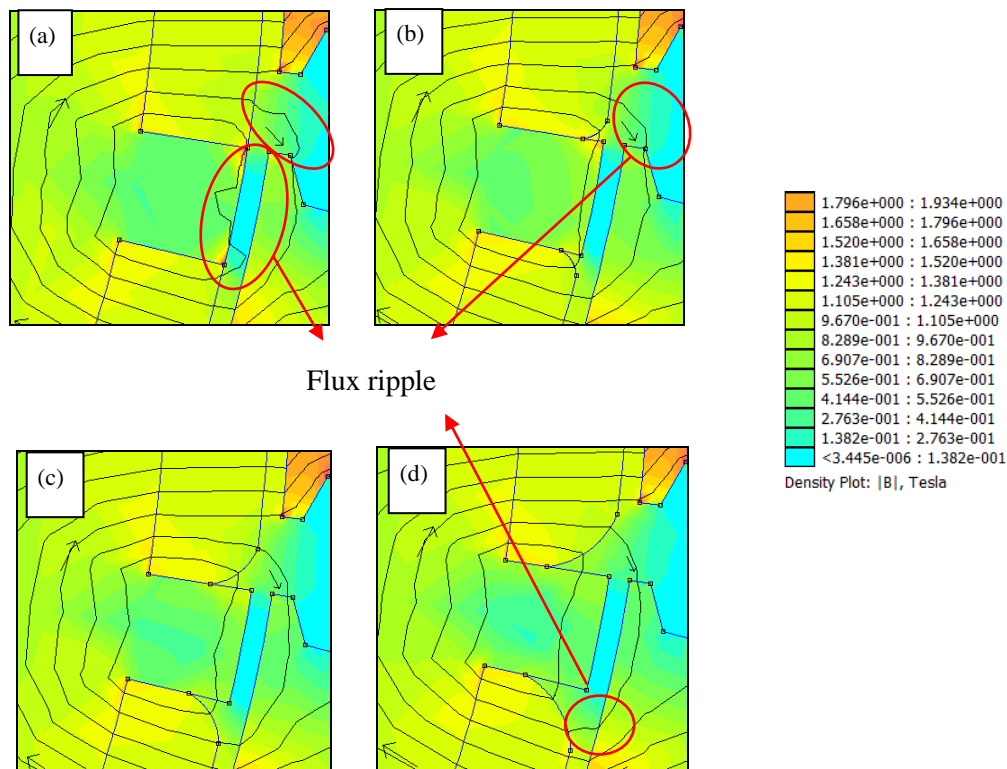


Figure 5 The contour map of flux density of RFIPM generator simulated by FEMM 4.2, (a) basic model; (b) ERM 1; (c) ERM 2; (d) ERM 3

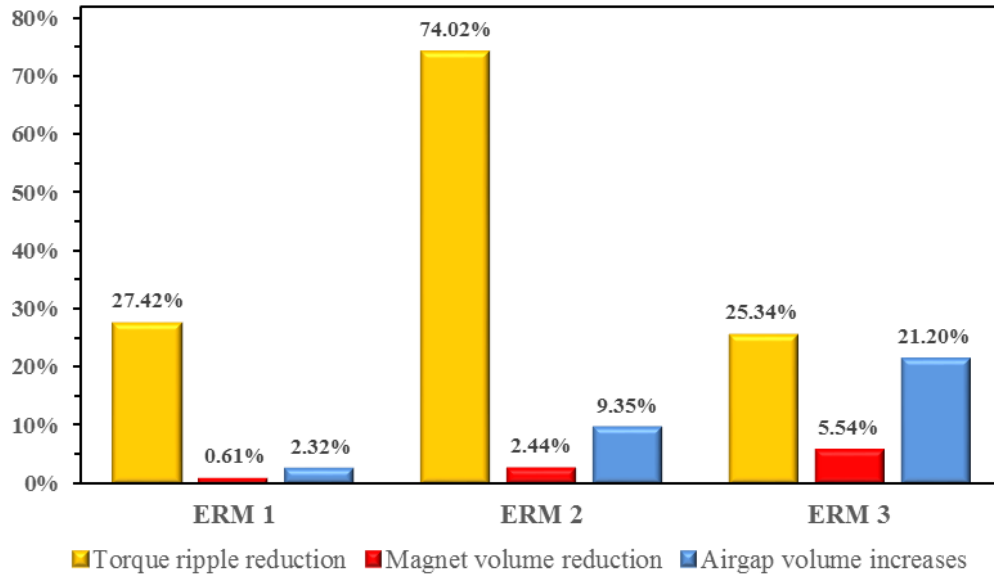


Figure 6 Comparison of torque ripple and magnet volume reduction and the increases in the air gap volume

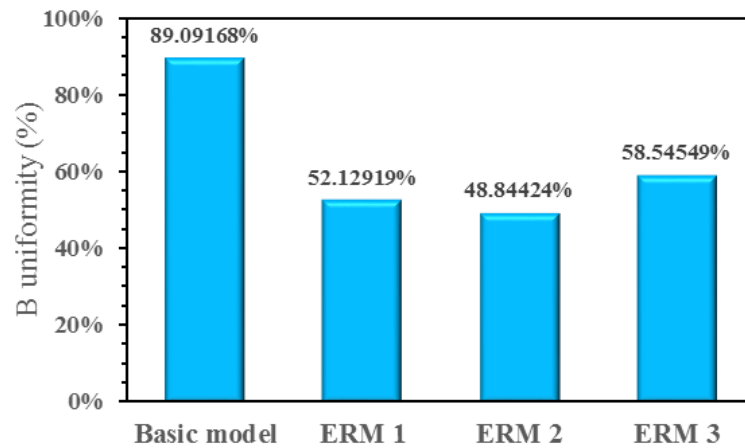


Figure 7 Comparison of flux density uniformity in air-gap

Torque generation has been fundamentally described by Maxwell's stress tensor, which illustrates well the fundamental principle of torque generation. This method is expressed as follows:

$$T = \frac{l}{\mu_0(r_{si} - r_{ro})} \int_S r B_n B_{tan} dS \quad (8)$$

where l is the length, B_n and B_{tan} denote the radial and tangential flux densities in the elements of surface S and formed between radii r_{ro} and r_{si} , and dS is the surface of one element.

According to Equation 8, we conclude that the electromagnetic torque is significantly affected by the geometry of both the rotor and stator as well as the flux density of the generator. In our approach, the r_{ro} of ERM was slightly decreased because of the cutting/material removal of the permanent magnets. Consequently, $r_{si} - r_{ro}$ would be larger, leading to a lower torque T . Moreover, the non-homogenous profiles of flux density over the surface in the air-gap of the

RFIPM generator may deteriorate the torque distribution. These phenomena are well-matched with the results simulated by FEMM 4.2.

5. CONCLUSION

This study investigated the effects of edge-rounded magnet poles on the torque ripple reduction and flux density uniformity in an RFIPM generator. Using FEMM 4.2, we simulated the electromagnetic torque of three different magnet shapes with edge-rounding techniques. We found that ERM 2 showed the lowest torque ripple (7.76%), the smoothest flux line, and the best flux density uniformity (48.8%). These phenomena were closely correlated with the optimized volume of the air-gap and the magnet volume, leading to better performance of the RFIPM generator.

6. ACKNOWLEDGMENT

The authors are grateful for the financial support provided by Universitas Indonesia through the 2017 PITTA (No. 831/UN2.R3.1/HKP.05.00/2017) funding scheme managed by the directorate for Research and Community Engagement (DRPM). C. Hudaya is grateful for the support of World-Class Professor Program, Faculty of Engineering - Universitas Indonesia funded by Ministry of Research, Technology and Higher Education of Republic of Indonesia.

7. REFERENCES

- Ahsanullah, K., Dutta, R., Fletcher, J., Rahman, M.F., 2013. Design of an Interior Permanent Magnet Synchronous Machine Suitable for Direct Drive Wind Turbine. *In: Renewable Power Generation Conference (RPG 2013)*, 2nd IET, 9–11 Sept. 2013, pp. 1–4
- Alberti, L., Barcaro, M., Bianchi, N., 2014. Design of a Low-Torque-Ripple Fractional-Slot Interior Permanent-Magnet Motor. *IEEE Transactions on Industry Applications*, Volume 50, pp. 1801–1808
- Baek, J., Bonthu, S.S.R., Kwak, S., Choi, S., 2014. Optimal Design of Five-phase Permanent Magnet Assisted Synchronous Reluctance Motor for Low Output Torque Ripple. *Energy Conversion Congress and Exposition (ECCE), IEEE*, pp. 2418–2424
- Dajaku, G., Gerling, D., 2014. New Methods for Reducing the Cogging Torque and Torque Ripples of PMSM. *In: Electric Drives Production Conference (EDPC)*, 4th International, Sept. 30-Oct. 1 2014, pp. 1–7
- Daohan, W., Xiuhe, W., Sang-Yong, J., 2013. Cogging Torque Minimization and Torque Ripple Suppression in Surface-mounted Permanent Magnet Synchronous Machines using Different Magnet Widths. *IEEE Transactions on Magnetics*, Volume 49, pp. 2295–2298
- Gasc, L., Fadel, M., Astier, S., Calejari, L., 2003. Load Torque Observer for Minimising Torque Ripple in PMSM. *In: Sixth International Conference on Electrical Machines and Systems. ICEMS 2003*, 9-11 Nov. 2003, Volume 2, pp. 473–476
- Gieras, J.F., 2010. *Third Edition Permanent Magnet Motor Technology: Design and Application*. New York, USA, CRC Press
- Gyeong-Chan, L., Seung-Han, K., Tae-Uk, J., 2014. Design on Permanent Magnet Structure of Radial Flux Permanent Magnet Generator for Cogging Torque Reduction and Low Torque Ripple. *In: 16th European Conference on Power Electronics and Applications (EPE'14-ECCE Europe)*, 26-28 Aug. 2014, pp. 1–9
- Husain, I., 2002. Minimization of Torque Ripple in SRM drives. *IEEE Transactions on Industrial Electronics*, Volume 49, pp. 28–39
- Handini, W., Setiabudy, R., Gunawan, R., 2016. Minimization of Torque Ripple in 24-slot 16-pole Inset Permanent Magnet Generator by Edge-rounded Magnet Poles and Stator Teeth

- Notch Techniques. *Journal of Theoretical and Applied Information Technology*, Volume 93(1). pp. 10–16
- Islam, R., Husain, I., Fardoun, A., Mclaughlin, K., 2009. Permanent-magnet Synchronous Motor Magnet Designs with Skewing for Torque Ripple and Cogging Torque Reduction. *IEEE Transactions on Industry Applications*, Volume 45, pp. 152–160
- Jiang, W., Reddy, P.B., Jahns, T.M., Lipo, T.A., Anbarasu, R., Sorensen, H.L., Osama, M., Skov Jensen, M.V.R., 2014. Segmented Permanent Magnet Synchronous Machines for Wind Energy Conversion System. *In: Power Electronics and Machines for Wind and Water Applications (PEMWA)*, 2014 IEEE Symposium, pp.1–8
- Ki-Chan, K., 2014. A Novel Method for Minimization of Cogging Torque and Torque Ripple for Interior Permanent Magnet Synchronous Motor. *IEEE Transactions on Magnetics*, Volume 50, pp. 793–796
- Kyung-Sik, S., Yong-Jae, K., Sang-Yong, J., 2014. Stator Teeth Shape Design for Torque Ripple Reduction in Surface-mounted Permanent Magnet Synchronous Motor. *In: 17th International Conference on Electrical Machines and Systems (ICEMS)*, 22-25 Oct. 2014, pp. 387–390
- Meier, F., 2008. Permanent-Magnet Synchronous Machines with Non-overlapping Concentrated Winding for Low-speed Direct Drive Applications. *Ph.D Thesis*, Royal Institute of Technology (KTH)
- Nur, T., Haroen, Y., 2014. Investigation the Influence of Magnet Slots with Fixed Slot Opening Width on the Cogging Torque of Inset-PMSM. *In: 2014 International Conference on Power Engineering and Renewable Energy (ICPERE)*, 9-11 Dec. 2014, pp. 195–197
- Sunan, E., Raza, K.S. M., Goto, H., Hai-Jiao, G., Ichinokur, O., 2010. Instantaneous Torque Ripple Control and Maximum Power Extraction in a Permanent Magnet Reluctance Generator Driven Wind Energy Conversion System. *In: XIX International Conference on Electrical Machines (ICEM)*, 6-8 Sept. 2010, pp. 1–6
- Upadhayay, P., Rajagopal, K.R., 2013. Torque Ripple Reduction using Magnet Pole Shaping in a Surface Mounted Permanent Magnet BLDC Motor. *In: International Conference on Renewable Energy Research and Applications (ICRERA)*, 20-23 Oct. 2013, pp.516–521
- Weizhong, F., Luk, P.C.K., Xin, S.J., Bin, X., Yu, W., 2011. Permanent-Magnet Flux-Switching Integrated Starter Generator with Different Rotor Configurations for Cogging Torque and Torque Ripple Mitigations. *IEEE Transactions on Industry Applications*, Volume 47, pp. 1247–1256
- Yicheng, C., Pillay, P., Khan, A., 2005. PM Wind Generator Topologies. *IEEE Transactions on Industry Applications*, Volume 41, pp. 1619–1626